

# Experimental Investigation of Phase Distributions of Two-phase Air-silicone Oil Flow in a Vertical Pipe

M. Abdulkadir, V. Hernandez-Perez, S. Sharaf, I. S. Lowndes\* and B. J. Azzopardi

**Abstract**—This paper reports the results of an experimental study conducted to characterise the gas-liquid multiphase flows experienced within a vertical riser transporting a range of gas-liquid flow rates. The scale experiments were performed using an air/silicone oil mixture within a 6 m long riser. The superficial air velocities studied ranged from 0.047 to 2.836 m/s, whilst maintaining a liquid superficial velocity at 0.047 m/s. Measurements of the mean cross-sectional and time average radial void fraction were obtained using a wire mesh sensor (WMS). The data were recorded at an acquisition frequency of 1000 Hz over an interval of 60 seconds. For the range of flow conditions studied, the average void fraction was observed to vary between 0.1 and 0.9. An analysis of the data collected concluded that the observed void fraction was strongly affected by the superficial gas velocity, whereby the higher the superficial gas velocity, the higher was the observed average void fraction. The average void fraction distributions observed were in good agreement with the results obtained by other researchers. When the air-silicone oil flows were fully developed reasonably symmetric profiles were observed, with the shape of the symmetry profile being strongly dependent on the superficial gas velocity.

**Keywords**—WMS, phase distribution, silicone-oil, riser

## I. INTRODUCTION

THE onshore and offshore production and transportation of oil and gas resources has always been a challenge within the energy industry, with engineers having to deal with the various technical and environmental challenges associated with multiphase flows.

For example, in an offshore environment, it is economically preferable to transport gas and liquid mixtures through a single flow line and separate them onshore.

However, the presence of two-phase flow can cause flow instability problems and may ultimately damage the pipe system itself [1]. The complexity of the potential flow regimes present within these pipelines has attracted considerable research interest to improve our understanding of two-phase flow behaviour in a pipe system under various processing conditions. Despite the importance of multiphase flows, their understanding is limited compared to that of single phase flows. In particular it is desirable to predict the relative concentrations of the different phases in the multiphase flows. Thus the need to identify and understand the basic scientific principles and fundamental processes which underlie the behaviour of these systems represents the motivation for this work. The research work presented in this paper is concerned only with gas-liquid flows in risers with particular interest towards oil and gas industry applications.

## II. BACKGROUND TO THE RESEARCH

Gardner and Neller [2] conducted an experimental study to investigate the distribution and redistribution of the multiphase flow phenomena observed in air-water flow systems. They used a traversing probe to measure the time averaged void fraction at any point over a range of chosen cross-sections. They concluded that reasonably symmetric air concentration profiles were obtained at a distance of 3.3 m from the mixing section. However, they did not investigate the influence of superficial gas velocity on flow development and symmetry.

Ohnuki and Akimoto [3] studied the effect of air injection methods on the development of air-water two-phase flows along a 0.48 m internal diameter and 2.016 m height vertical pipe. The two injection methods, porous sinter and nozzle injection, were used to obtain different flow structures in the developing region. From an analysis of their experimental data they found that no air slugs occupying the flow path were recognised regardless of the air injection methods even under the condition where slug flow is realized in the small-scale pipe. That the lower half of the test section was affected by the air injection method, whilst for the upper half of the test section, the effects of the air injection methods observed were small. Later, they [4] extended their earlier work to studying the transition of flow pattern and phase distributions in the upward air-water flows observed along a 0.2 m internal diameter and 12.3 m height vertical pipe. They observed flow patterns and recorded measurements of axial differential pressure, phase distribution, bubble size and bubble and water

M. Abdulkadir is a PhD student in the Process and Environmental Engineering Research Division, University of Nottingham.

V. Hernandez-Perez is a research fellow in the Process and Environmental Engineering Research Division, University of Nottingham.

S. Sharaf is a PhD student in the Process and Environmental Engineering Research Division, University of Nottingham

I. S. Lowndes, the corresponding author, is an Associate Professor and Reader in Environmental Engineering at the Faculty of Engineering, University of Nottingham. Email address: ian.lowndes@nottingham.ac.uk

B. J. Azzopardi is Lady Trent Professor and Head of the Department of Chemical and Environmental Engineering, University of Nottingham.

velocities. They compared the data of other workers with their experimental data. They concluded that further detailed measurements were needed to investigate the flow structure under the agitated bubbly flow.

Shen et al. [5] studied two-phase distribution in a vertical (0.2 m internal diameter and height 24 m) pipe. They used optical probes and pressure transducers to record local measurements including; void fraction, Sauter mean diameter and pressure loss. From an analysis of their experimental data they concluded that the phase distribution patterns could be subdivided into basic patterns, namely, wall peak and core peak using the concept of Fisher skewness. However, the weakness of Fisher skewness is its sensitivity to irregular observations at the extremes where the difference between the mean and the value is cubed.

Later, Azzopardi et al [6] carried out wire mesh sensor studies in a vertical 67 mm internal diameter pipe using air-water as the operating fluids. They measured the radial time averaged void fraction and cross-sectional average time series of void fraction. They determined that the wire mesh sensor was capable of providing insight into the details of phase distributions in a pipe. They expressed the cross-sectional time averaged air void fraction in terms of the gas mass fraction. Also, these studies were restricted to the use of air-water flow mixtures.

The objectives of the experimental studies reported in this paper were to investigate the multiphase flow phenomena observed on the transport of air-silicone mixtures in a vertical pipe. Experimental studies have been conducted on a vertical 67 mm internal diameter vertical riser. A wire-mesh sensor (WMS) was devised for air-silicone oil to measure mean cross-sectional void fraction and time averaged radial void fraction. The WMS was based on capacitance measurements

and works with non-conductive materials such as silicone oil. Data obtained in these facilities was used to identify the phase distributions in a vertical riser in a quantitative manner.

### III. EXPERIMENTAL ARRANGEMENTS

This section presents an outline of the construction of the experimental rig used to study gas-liquid flow behaviour in a vertical riser. An overview of the experimental facility is given in section 2.1 and section 2.2 describes the capacitance wire mesh sensor (WMS)

#### A. Overview of the facility

All experiments were carried out on an inclinable rig in the Chemical Engineering Laboratory of the department of Chemical and Environmental engineering at University of Nottingham. The experimental facility used which had been employed earlier for annular flow studies by [7], [8] and [9] and has been employed for two phase flow in inclinable pipes by [10]. The experimental facility consists of a main testing section of the rig made from transparent acrylic glass pipes of 0.067 m inside diameter and 6 m to observe flow development over testing section. This testing section is made up of shorter pipes. Each shorter pipe can be easily installed or replaced. For all experiments, the testing pipe was maintained at 6 m long from mixing section to make sure that it was long enough for flow development. The testing pipe is set up so that it can be inclined from  $-5^\circ$  to  $90^\circ$  and it is mounted on a rigid steel frame which could be positioned in intervals of 5 degrees, to enable the investigation of influence of different inclinations on flow regimes.

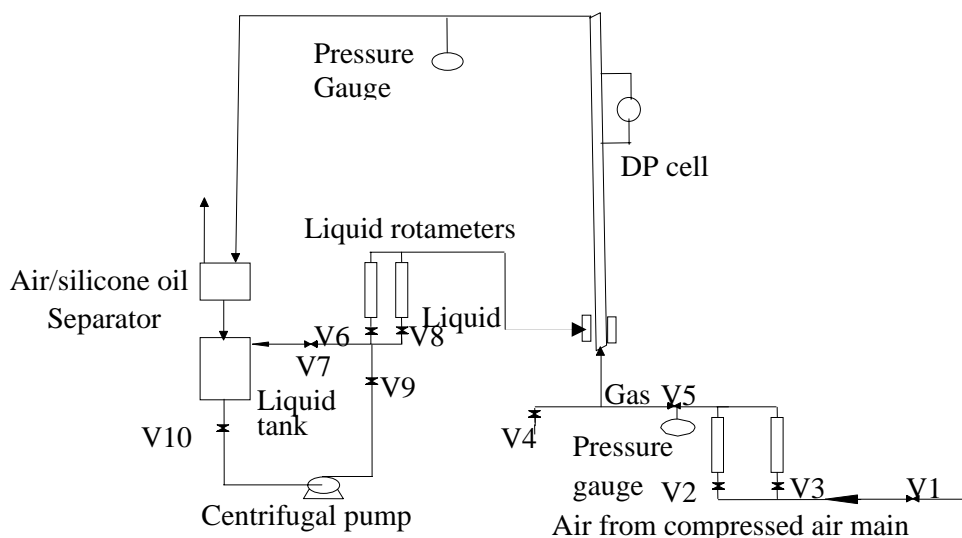


Fig. 1: Schematic diagram of vertical rig. This rig was instrumental to take physical measurements that could be used to characterise the flow regime existing the vertical pipe when the flow rates of both the oil and the air injection were varied.

Air is supplied from compressed air main supply at 3.2 barg through valve (V1). It was measured by two parallel air flow rotameters and is controlled by valves (V2) and (V3) as shown in Fig. 1. The two rotameters used have a maximum range of flow rates of 100 l/ min and 1000 l/ min, respectively. An air distributor whose function it is to make sure that all of the air coming into the pipe is well mixed and equally distributed through the cross section of the pipe is installed at the centre of the mixing section. Valve (V5) is placed after the pressure gauge, which when closed prevents liquid from going through the air line to the rotameters. In addition, the pressures were measured prior to entering the mixing section. Liquid was stored in a liquid storage tank and it was pumped by using a centrifugal pump. Valve (V7) is a bypass valve which helps to control the circulation of the liquid. Two parallel liquid rotameters were installed to measure liquid flow rate coming into the testing section pipe. The liquid flow rate is controlled by valves (V6) and (V8). After coming out from the testing section pipe, the air-liquid mixture enters into the separator. In the separator air is released to the atmosphere from the top of the separator and liquid is settled under the influence of gravity and flows through the bottom to return to main liquid tank. Valve (V4) is installed to drain the liquid in the testing section tube.

In this present work, the inclinable rig was converted to a vertical riser as shown in Fig. 1. This rig used an air-silicone oil mixture to examine the behaviour of gas-liquid flows in a vertical riser using a state of the arts instrument called wire mesh sensor (WMS). The WMS is able to measure the difference in the electrical capacitance of both phases. The sensor is built into an acrylic resin frame supports which allows it to be mounted in the test pipe. The WMS was placed at about 5.15 m away from the mixing section. It consists of two planes of 24 stainless steel wires with 0.12 mm diameter, 2.78 mm wire separation within each plane and 2 mm axial plane distance. This determined the spatio/ temporal resolution of the sensor. Since the square sensor is installed in a circular tube, only 440 of the total 576 wire crossing points are within the radius of the tube. During the experiments, the horizontal transmitter lines are pulsed one after another. By measuring the signal of all crossing vertical receiver wires, the local capacitance around the crossing points in the mesh is known. This capacitance signal is a measure for the amount of silicone oil, and thus indicates the local phase composition in the grid cell. The data were taken at a data acquisition frequency of 1000 Hz over an interval of 60 seconds.

TABLE I PROPERTIES OF THE FLUIDS

Fluid	Density (kg/ m <sup>3</sup> )	Viscosity (kg/ ms)	Surface tension (N/ m)
Air	1.18	0.000018	

Silicone oil	900	0.0053	0.02
--------------	-----	--------	------

In the present study, it is mainly time varying cross-sectional void fractions and time averaged radial void fractions that have been used for extracting the information on flow pattern and phase distributions in a quantitative manner. The experiments were performed at room temperatures (15-20°C). The properties of the two fluids used in the experiments are as shown in Table 1.

#### B. Description of the Wire Mesh Sensor (WMS)

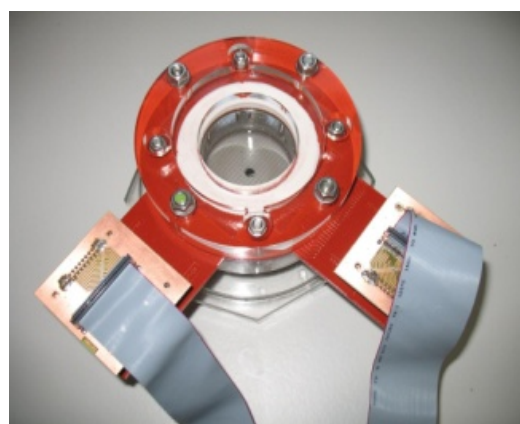


Fig. 2: Wire mesh sensor (WMS)

In order to obtain quantitative information on the flow, both time and cross-sectional averaging of the void fraction data were used, as explained in [11]. The averaging was based on weight coefficients that define the contribution of each crossing point of wires ( $i, j$ ) in the sensor matrix to the size of the domain, over which the averaging had to be done. The definition of the weight coefficients ( $a_{i,j}$ ) necessary to obtain a cross-section averaged void fraction is shown in Fig. 3. The averaging was done by calculating for each sampling period individually:

$$\bar{\varepsilon} = \varepsilon(t) = \sum_i \sum_j a_{i,j} \cdot \varepsilon_{i,j,k} \quad (1)$$

Radial time averaged void fraction were calculated by averaging the local instantaneous void fractions over the measurement period and over a number of ring-shaped domains (m). This is done by the following equation:

$$\bar{\varepsilon} = \frac{1}{k_{\max}} \sum_k \sum_i \sum_j a_{i,j,m} \cdot \varepsilon_{i,j,k} \quad (2)$$

where,

$a_{i,j,m}$  are the weight coefficients denoting the contribution of each measurement point with the indexes  $i, j$  to a ring with the number  $m$ . This ring-shaped averaging domain covers a given radial distance from the centre of the sensor as shown in Fig. 4.

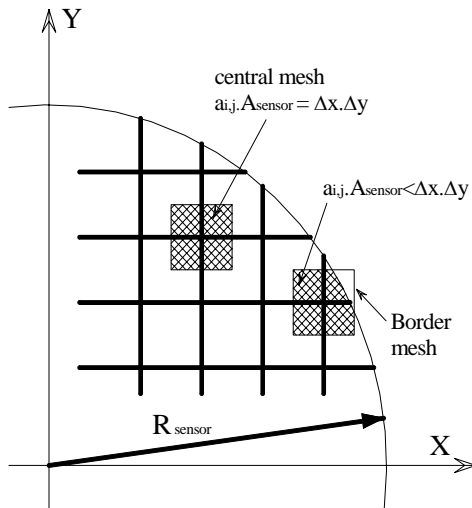


Fig. 3: Weight coefficients for the cross-section averaging of local void fractions measured by the WMS

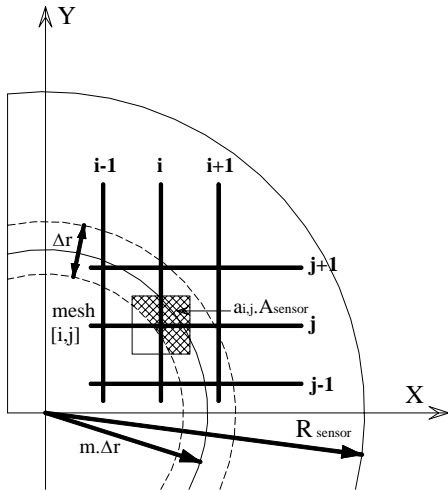
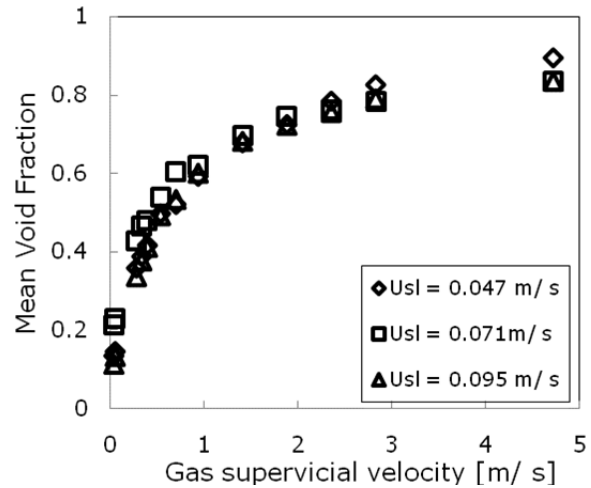


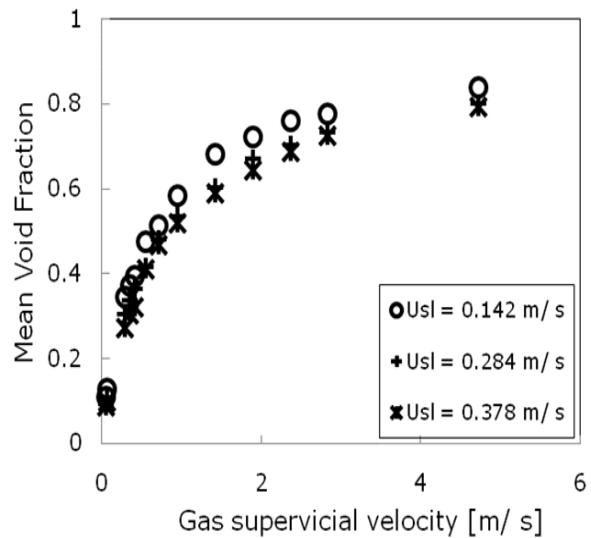
Fig. 4: Weights coefficients for the cross-section averaging of local void fractions over a number of ring-shaped domains.

## V. RESULTS AND DISCUSSION

This section presents a comparison of the mean void fraction distribution obtained over a range of different superficial gas velocities. It will also compare the radial time averaged void fraction (%) for all cross points ( $24 \times 24$  values) of the WMS from axis of pipe in (mm). Finally the probability density functions (PDF) of void fraction are presented.



(a)



(b)

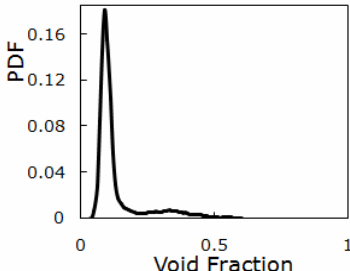
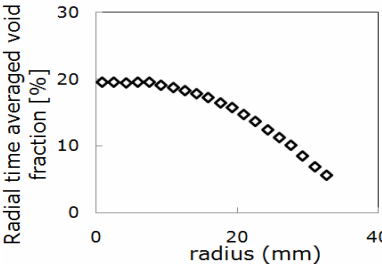
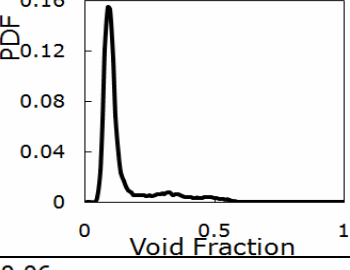
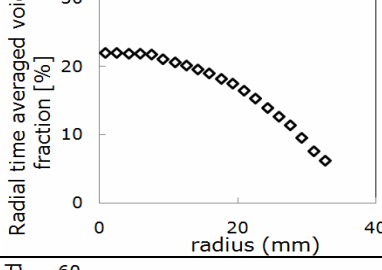
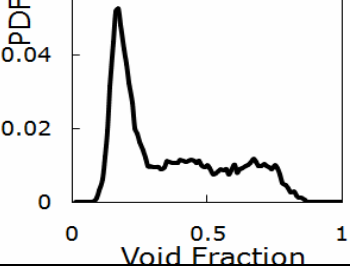
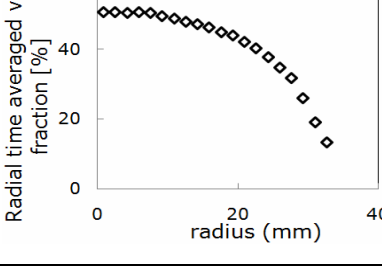
Fig. 5: Variation of void fraction distribution with superficial gas velocity at different liquid superficial velocities of (a)  $0.047 < U_{sl} < 0.095$  m/s (b)  $0.142 < U_{sl} < 0.378$  m/s

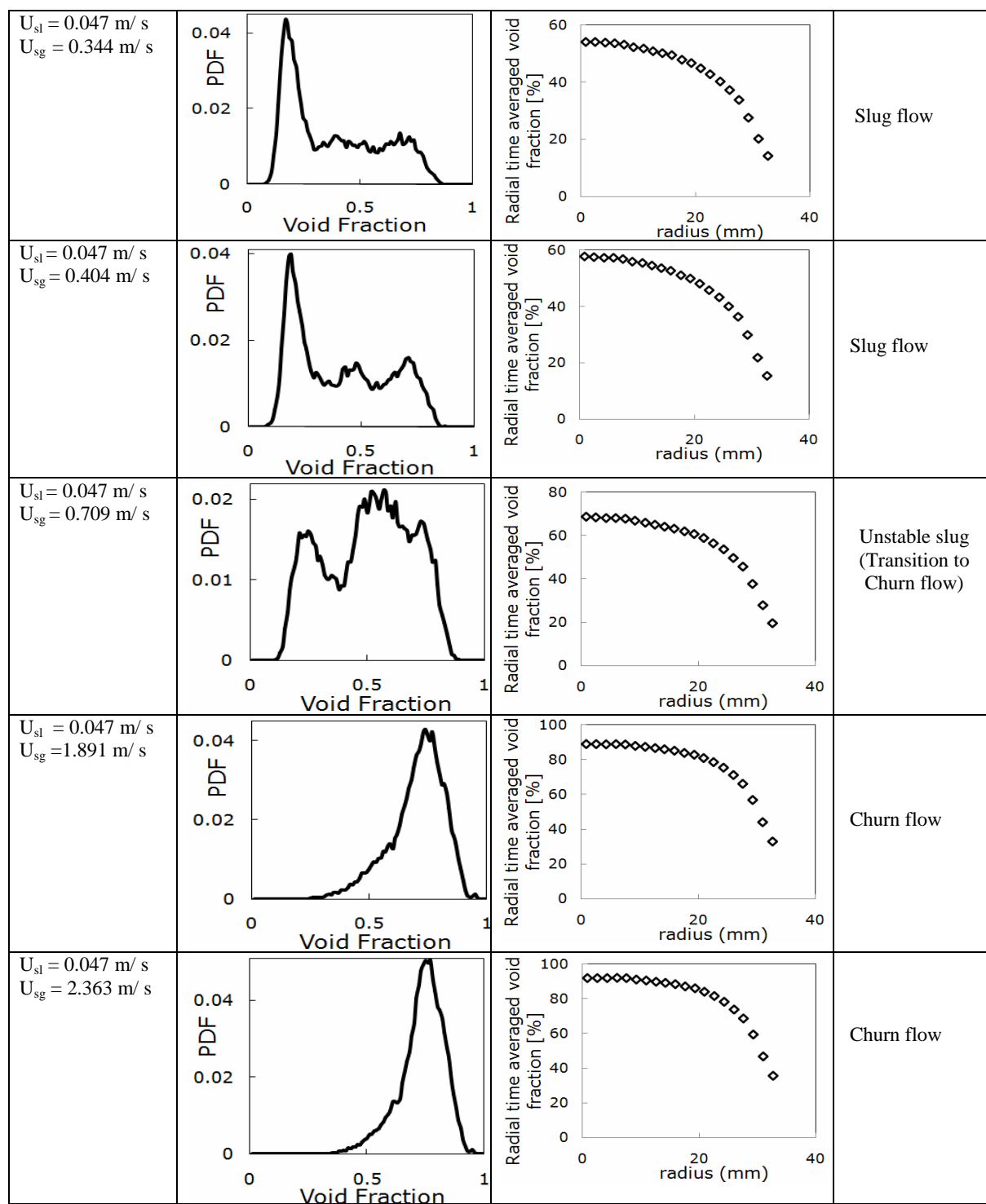
An examination of the data plotted on Fig. 5 concludes that all the plots of mean void fraction against superficial gas velocities followed the same trend. However, for a superficial

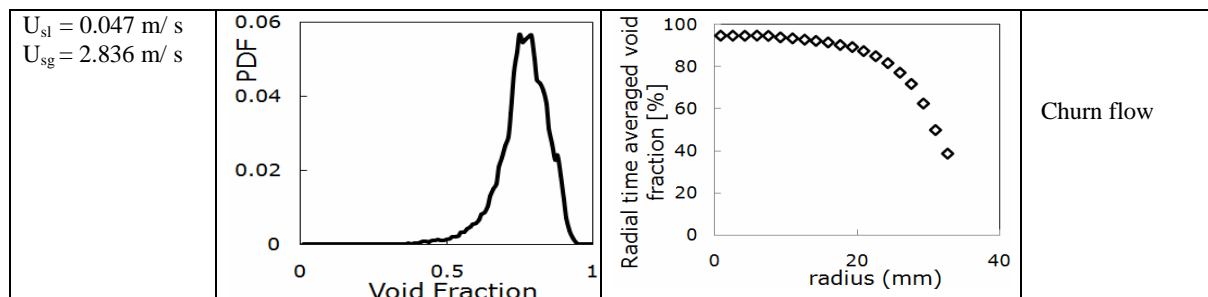
liquid velocity of 0.047 m/ s, the mean void fraction, started initially with 0.2 at a superficial gas velocity of 0.047 m/ s and extended to a maximum value of 0.896 at a superficial gas velocity of 4.727 m/ s. It also shows that for superficial liquid velocities of 0.07, 0.09 and 0.14 m/ s, the initial mean void fraction was 0.1 at a superficial gas velocity of 0.047 m/ s and reached same mean void fraction of 0.839 at a superficial gas velocity of 4.727 m/ s. For further superficial liquid velocities of 0.28 and 0.38 m/ s, a least mean void fraction of 0.794 was obtained at both superficial gas velocities of 4.727 m/ s though starting with a mean void fraction of 0.1 at a superficial gas velocity of 0.047 m/ s. These observations suggest that the relationship between mean void fraction and superficial gas

velocity follows the trend  $\varepsilon \propto U_{sg}^n$ , with the value of  $n$  depending on the degree of linearity. It can be observed that for almost all superficial liquid velocities, the relationship between mean void fraction and superficial gas velocity is almost linear, with  $n \approx 1$  occurring within a region of superficial gas velocities of 0.047, 0.061 and 0.288 m/ s. For an increase of superficial gas velocities from 0.288 to 2.836 m/ s, the relationship deviates from linearity with  $n \approx 0.8$ . With a further increase of superficial gas velocity from 2.836 to 4.727 m/ s, the trend is linear, with  $n \approx 1$ .

TABLE II PROBABILITY DENSITY FUNCTION (PDF) OF VOID FRACTION, RADIAL TIME AVERAGED VOID FRACTIONS AND FLOW PATTERN AT DIFFERENT AIR SUPERFICIAL VELOCITIES

Flow conditions	PDF	Time averaged radial void fraction [%]	Flow pattern
$U_{sl} = 0.047$ m/ s $U_{sg} = 0.047$ m/ s			Spherical cap bubble
$U_{sl} = 0.047$ m/ s $U_{sg} = 0.061$ m/ s			Spherical cap bubble
$U_{sl} = 0.047$ m/ s $U_{sg} = 0.288$ m/ s			Slug flow





It can be observed from Table 2, column 3 that at superficial liquid velocity of  $0.047 \text{ m/s}$  and superficial gas velocities of  $0.047 < U_{sg} < 2.836 \text{ m/s}$ , parabolic profiles are obtained. The profiles show that maximum and minimum radial void fraction are observed at the centre of the pipe and pipe wall respectively. The maximum radial void fraction as observed from Table 2 rows 1 to 9 are 19.602, 22.005, 50.764, 54.194, 57.698, 65.375, 88.862, 91.837, and 94.582 % respectively. The profiles then moved downwards in a parabolic manner to a definite minimum. The minimum radial void fractions so obtained are 5.626, 6.221, 13.443, 14.18, 15.33, 17.938, 32.911, 35.579, and 38.61 % respectively. The maximum and minimum % radial void fraction occurred at 0.8 and 32.7 mm respectively. The profiles obtained are in good agreement with the results obtained by [3]. The results therefore, show that an increase in superficial gas velocity is responsible for an increase in radial void fraction at the centre of the pipe and pipe wall. It is worthy of mention that column 3, rows 7 to 9, that the profiles started becoming flattened at the top as the air superficial velocity increased, thus, giving impression that the plots resembled turbulent flow profiles. The profiles obtained are in good agreement with the results obtained by [2], [12] and [13] and contrary to the results obtained by [4]. The results show that the shape of the symmetry and an increase in % void fraction are dependent on air superficial velocity as shown in Fig. 5.

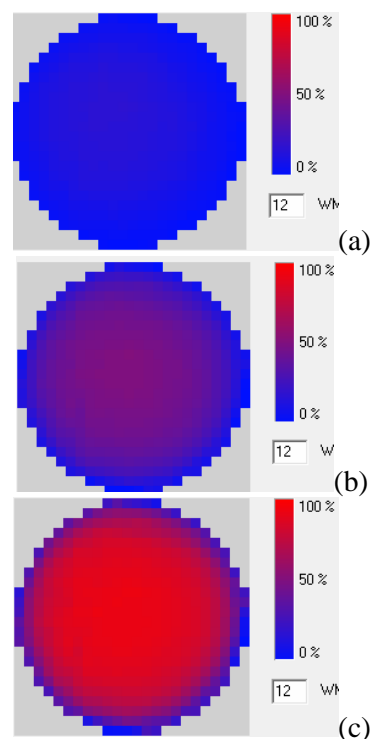


Fig. 6: Contours of cross-sectional void fraction at (a)  $U_{sl} = 0.047 \text{ m/s}$  and  $U_{sg} = 0.047 \text{ m/s}$  (b)  $U_{sl} = 0.047 \text{ m/s}$  and  $U_{sg} = 0.404 \text{ m/s}$  (c)  $U_{sl} = 0.047 \text{ m/s}$  and  $U_{sg} = 2.836 \text{ m/s}$ . The contours confirm that the profiles are indeed symmetrical

Time varying void fraction data and probability density function (PDF) distributions are used to discriminate between the various flow patterns according to Costigan and Whalley [14] who defined a single peak PDF existing at low void fraction with a broadening tail as spherical cap bubble and twin peaked PDFs of recorded void fractions as slug flow. Also that high void fraction peak with a broadening tail corresponds to churn flow.

The PDF of void fraction from Table 2 column 1 show that the observed flow patterns are spherical cap bubble, slug and churn flows. Column 3, rows 1 and 2 which were observed to

be at lower void fraction fell under the spherical cap bubble as represented by column 2 rows 1 and 2. However, the observed symmetric profiles in column 3, rows 3 to 6 can be classified as shown in column 2 rows 3 to 6 as slug flows. The symmetric profiles, though with a flattened front as observed in column 3, rows 7 to 9 can be represented as churn flows as shown in column 2, rows 7 to 9.

## VI. CONCLUSION

Comparison of variation of overall average void fraction as a function of air superficial velocity for  $U_{sl} \leq 0.378$  m/s was carried out. The results show that all exhibited same trend. Although, for superficial liquid velocity of 0.047 m/s which produced the maximum average void fraction started initially with of 0.2 and finally peaked at 0.9. While the least value of average void fraction was obtained from both superficial liquid velocities of 0.284 and 0.378 m/s. Though, both initially started with an average void fraction of 0.1 and thereafter peaked at 0.78. The results therefore show that the trend can be represented as,  $\varepsilon \alpha U_{sg}^n$  with n depending on the degree of linearity. The results of the analysis also showed that reasonably symmetric profiles were obtained when the air-silicone oil was fully developed and that the shape of the profile was strongly dependent on superficial gas velocity. The results also showed that low and high void fraction symmetric parabolic profiles can be represented as spherical cap bubble and slug flows respectively. However, flattened symmetric profile can be represented as churn flow. The analysis therefore showed that the WMS was capable of providing excellent data for mean cross-sectional and time average radial void fraction.

## NOMENCLATURE

Symbol	Description, Units
$\bar{\varepsilon}$	Averaged void fraction, %
$\varepsilon_t$	Time varying void fraction, %
$\alpha$	Proportionality, dimensionless
$\Sigma$	Summation, dimensionless
$\varepsilon$	Void fraction, %
$n$	The degree of linearity, dimensionless
$U_{sg}$	Gas superficial velocity, m/s
$U_{sl}$	Liquid superficial velocity, m/s

## ACKNOWLEDGEMENT

M. Abdulkadir would like to express sincere appreciation to the Nigerian government through the Petroleum Technology

Development Fund (PTDF) for providing the funding for his doctoral studies.

V. Hernandez Perez and S. Sharaf are funded by EPSRC under grant EP/F016050/1.

This work has been undertaken within the Joint Project on Transient Multiphase Flows and Flow Assurance. The Author(s) wish to acknowledge the contributions made to this project by the UK Engineering and Physical Sciences Research Council (EPSRC) and the following: - GL Industrial Services; BP Exploration; CD-adapco; Chevron; ConocoPhillips; ENI; ExxonMobil; FEESA; IFP; Institutt for Energiteknikk; PDVSA (INTEVEP); Petrobras; PETRONAS; SPT; Shell; SINTEF; Statoil and TOTAL. The Author(s) wish to express their sincere gratitude for this support.

## REFERENCES

- [1] Abdulkadir, M., Zhao, D., Sharaf, S., Abdulkareem, L.S., Lowndes, I.S., Azzopardi, B.J., 2010, Interrogating the effect of bends on gas-liquid flow using advanced instrumentation, ICMF 2010, 7<sup>th</sup> International Conference on Multiphase Flow, Tampa, FL, USA. (Accepted)
- [2] Gardner, G. C., and Neller, P. H., 1969, Phase distributions flow of an air-water mixture round bends and past obstructions, Proc. Inst. Mech. Engr., Vol. 184, No. 3C, pp. 93 -101
- [3] Ohnuki, A. and Akimoto, H. (1996), An experimental study on developing air -water two-phase flow along a large vertical pipe: Effect of air injection method, Int. J. Multiphase Flow, Vol. 22, No. 6, pp. 1143-1154.
- [4] Ohnuki, A. and Akimoto, H. (2000), Experimental study on transition of flow pattern and phase distribution in upward air-water two-phase flow along a large vertical pipe, Int. J. Multiphase Flow, Vol. 26, No. 3, pp. 367-386.
- [5] Shen, X., Mishima, K., and Nakamura, H. (2004), Two-phase distribution in a vertical large diameter pipe, Int. J. Heat and Mass Transfer, Vol. 48, pp. 211-225
- [6] Azzopardi, B. J., Hernandez Perez, V., Kaji, R., Da Silva, M. J., Beyer, M., and Hampel, U., 2008, Wire mesh sensor studies in a vertical pipe, HEAT 2008, Fifth International Conference on Multiphase Systems, Bialystok, Poland.
- [7] Azzopardi, B. J., 1997, Drops in annular two-phase flow, International Journal of Multiphase Flow, Vol. 23, pp. 1-53.
- [8] Geraci, G., Azzopardi, B. J., and Van Maanen, H.R.E., 2007a, Inclination effects on circumferential film distribution in annular gas/liquid flows, AIChE Journal, Vol. 53, No.5, pp. 1144-1150.
- [9] Geraci, G., Azzopardi, B. J., and Van Maanen, H.R.E., 2007b, Effects of inclination on circumferential film thickness variation in annular gas/liquid flows, Chemical Engineering Science, Vol. 62, No.11, pp. 3032-3042.
- [10] Hernandez-Perez, V., 2007, Gas-liquid two-phase flow in inclined pipes, a PhD Thesis, University of Nottingham, United Kingdom
- [11] Prasser, H.M., Krepper, E. and Lucas, D., Evolution of the two-phase flow in a vertical tube—decomposition of gas fraction profiles according to bubble size classes using wire-mesh sensors, Int. J. Therm. Sci. 41 (2002) 17–28
- [12] Carver, M. B., 1984, Numerical computation of phase separation in two fluid flow, ASME Paper No. 82-FE-2, Vol. 106/ 153
- [13] Carver, M.B., and Salcudean, M., 1986, Three-dimensional numerical modelling of phase distribution of two - fluid flow in elbows and return bends, Numerical Heat Transfer, Vol. 10, pp. 229-251
- [14] Costigan, G., and Whalley, P. B., 1996, Slug flow regime identification from dynamic void fraction measurements in vertical air-water flows. Int. J. Multiphase Flow, Vol. 23, No. 2, pp. 263-282